Measurement report: Characteristics of nitrogen-containing organics in $PM_{2.5}$ in Urumqi, northwest China: differential impacts of combustion of fresh and old-age biomass materials

Yi-Jia Ma[1], Yu Xu[2,*], Ting Yang[1], Hong-Wei Xiao[2], Hua-Yun Xiao[2]

[1]School of Environmental Science and Engineering, Shanghai Jiao Tong University, Shanghai 200240, China

[2]School of Agriculture and Biology, Shanghai Jiao Tong University, Shanghai 200240, China

*Corresponding authors

Yu Xu

E-mail: xuyu360@sjtu.edu.cn

Abstract: Nitrogen-containing organic compounds (NOCs) are abundant and important aerosol components deeply involved in the global nitrogen cycle. However, the sources and formation processes of NOCs remain largely unknown, particularly in the city (Urumqi, China) farthest from the ocean worldwide. Here, NOCs in $PM_{2.5}$ collected in Urumqi over a one-year period were characterized by ultrahigh-resolution mass spectrometry. The abundance of CHON compounds (mainly oxygen-poor unsaturated aliphatic-like species) in the positive ion mode was higher in the warm period than in the cold period, which was largely attributed to the contribution of fresh biomass material combustion (e.g., forest fires) associated with amidation of unsaturated fatty acids in the warm period, rather than the oxidation processes. However, CHON compounds (mainly nitro-aromatic species) in the negative ion mode increased significantly in the cold period, which was tightly related to old-age biomass combustion (e.g., dry straws) in wintertime Urumqi. For CHN compounds, alkyl nitriles and aromatic species showed higher abundance in the warm and cold periods, respectively. Alkyl nitriles can be derived from fresh biomass material combustion associated with the dehydration of amides (the main CHON compounds in the warm period). In contrast, aromatic species were tightly related to old-age biomass burning. These findings further suggested different impacts of the combustion of fresh- and old-age biomass materials on NOC compositions in different seasons. The overall results shed light on the mechanisms by which fresh and old-age biomass materials release different NOCs during combustion.

Keywords: Aerosols, Organic nitrogen, Molecular composition, Fresh biomass, Old-

age biomass

1. Introduction

Fine particulate matter ($PM_{2.5}$) is a typical atmospheric pollutant that can affect the global climate system, as well as urban air quality and human health (Seinfeld et al., 2016; Wang et al., 2021a). Organic aerosol (OA) contributes significantly (20–90%) to $PM_{2.5}$ mass concentration in most polluted areas worldwide (Zhang et al., 2007; Han et al., 2023). Up to 77% of molecules in OA include nitrogen-containing functional groups (Ditto et al., 2020; Kenagy et al., 2021), which have been suggested to play important roles in the formation, transformation, acidity, and hygroscopicity of OA (Xu et al., 2020; Wang et al., 2017b; Laskin et al., 2009). Moreover, the further oxidation or nitrification of some nitrogen-containing organic compounds (NOCs) and volatile organic compounds (VOCs) by ozone (O_3), hydroxyl radical (•OH), and nitrogen oxides (NO_x) can lead to an increase in the health hazards of OA (Franze et al., 2005; Bandowe and Meusel, 2017). Nitrated amino acids and nitrated PAHs are two representative hazard NOCs (Franze et al., 2005; Bandowe and Meusel, 2017). Thus, the identification of aerosol NOCs at the molecular level is important for improving our understanding of the precursors, sources, and formation processes of nitrogen-containing OA.

Previous observations in urban, rural, marine, and forest areas have suggested that the molecular composition and relative abundance of aerosol NOCs were spatially different (Samy and Hays, 2013; Jiang et al., 2022; Lin et al., 2012; Xu et al., 2023; Zeng et al., 2021; Zhang et al., 2022; Zeng et al., 2020). These differences can be mainly

attributed to the diverse sources and formation mechanisms of aerosol NOCs. Commonly reported primary sources include combustion process releases and natural emissions (e.g., soils, plant debris, pollen, and ocean) (Song et al., 2022; Wang et al., 2017b; Cape et al., 2011; Lin et al., 2023). In addition, aerosol NOCs can also be tightly associated with secondary formation processes involving the reactions of reactive nitrogen with VOCs or particle-phase CHO compounds (Bandowe and Meusel, 2017; Zarzana et al., 2012; Laskin et al., 2014). For example, laboratory experiments have found that the oxidation of isoprene and α-/β-pinene in the presence of NO_x can result in the formation of organic nitrates (e.g., methacryloyl peroxynitrate, dihydroxynitrates, and monohydroxynitrates) (Surratt et al., 2010; Rollins et al., 2012; Nguyen et al., 2015). The reduced nitrogen species (e.g., NH_3, NH_4^+, and organic amines) have been demonstrated to contribute to the formation of NOCs through "carbonyl-to-imine" transformations in the laboratory experiments (Zarzana et al., 2012; Laskin et al., 2014). In the field observation studies, NOCs in particulate matter were analyzed at the molecular level to indicate their sources and formation mechanisms (Jiang et al., 2022; Lin et al., 2012; Zhong et al., 2023). Xu et al. (2023) characterized the variations of molecular compositions in urban road $PM_{2.5}$, suggesting that organic nitrates increased largely through the interactions of atmospheric oxidants, reactive gas-phase organics, and aerosol liquid water. Several field studies conducted in Beijing (China) and Guangzhou (China) also suggested that the molecular compositions and formation of NOCs were tightly associated with environmental conditions (Jiang et al., 2022; Lin et al., 2012; Xie et al., 2020). Generally, most studies on aerosol NOCs were performed

in economically developed regions, as well as in forest and marine areas (Jiang et al., 2022; Wang et al., 2017a; Ditto et al., 2022b; Altieri et al., 2016; Xu et al., 2020; Liu et al., 2023; Zhang et al., 2022; Zeng et al., 2020).In contrast, few studies have investigated the sources and atmospheric transformation of NOCs in the northwest border urban of China (e.g., Urumqi) with fragile ecology and harsh environmental conditions (e.g., cold winter and dry summer), which may hinder our comprehensive and in-depth understanding of the formation process of NOCs in ambient aerosols.

Biomass burning emissions were widely reported in the source identification of aerosol NOCs in northern and southwestern China because of heating and cooking needs (Zhong et al., 2023; Wang et al., 2021c; Chen et al., 2017). A recent observation study in urban Tianjin suggested that most CHON compounds in wintertime $PM_{2.5}$ originated from biomass burning (Zhong et al., 2023). The CHN_2 compounds have been identified in biomass burning OA (BBOA) (Laskin et al., 2009; Wang et al., 2017b). Moreover, the high temperature generated by biomass burning can facilitate the release of ammonia, a process that caused the reaction of carboxylic acids (e.g., oleic acid) with ammonia to form amides and alkyl nitriles (Radzi Bin Abas et al., 2004; Simoneit et al., 2003). Interestingly, we found that biomass burning in rural China typically includes fresh biomass materials (e.g., forest fires) and old-age biomass materials (e.g., straw after autumn harvest, fallen leaf, and deadwood). Fresh biomass is rich in oils and proteins, whereas old-age biomass materials are usually oligotrophic due to the transfer of nutrients to tender tissues or fruits (Jian et al., 2016; Xu and Xiao, 2017). Thus, NOCs released from different types of biomass combustion may vary in molecular

compositions. However, there are large gaps in our current knowledge about the impacts of fresh and old-age biomass burning on NOCs in ambient aerosols.

Urumqi (northwest China) is the largest inland city farthest from the ocean in the world, which is becoming increasingly prominent due to the national strategy of the "One Belt, One Road." The city and neighboring countries have a dry summer that can easily trigger forest fires (Bátori et al., 2018; Xu et al., 2021), while the winter is freezing with intensive old-age biomass and fuel combustion for heating (Ren et al., 2017). In this study, we presented one-year ambient measurements of the chemical compositions in $PM_{2.5}$ collected from Urumqi. The specific aims of this study are (1) to investigate the molecular-level speciation of functionalized organic nitrogen compounds via high-resolution mass spectrometry with positive (ESI+) and negative (ESI−) ionizations and (2) to investigate the potential sources and formation processes for NOCs with a special focus on the relative influences of fresh and old-age biomass burning in different seasons.

2. Materials and methods

2.1. Study site description and sample collection

The study was conducted in Urumqi city, which has an average altitude of 800 m. The region has an arid temperate continental climate with an annual mean temperature of 7.4 ± 13.9 °C and an annual mean rainfall of 27.8 mm. The sampling site is located in the suburban area (Boda campus of Xinjiang University) of the city (87.75°E, 43.86°N) (**Figure S1**), which is characterized by low population and traffic density.

This is because Urumqi is relatively vast and sparsely populated compared to developed coastal cities in China (Qizhi et al., 2016). Additionally, the area is surrounded by mountains on three sides, resulting in the difficulty in diffusing air pollutants. The dominant forest trees in this area are *Picea schrenkiana*, *Betula tianschanica* Rupr., *Populus talassica* Kom., and *Ulmus pumila* L.. The dry climate and strong sunlight in the warm period (18.81 ± 6.4°C, **Table S1**) would be the main culprits of forest fires in the local and nearby areas. In the cold period (–1.96 ± 11.26°C) (**Table S1**), the centralized heating and old-age biomass burning may be the main contributors to local air pollution. Thus, it provides an unexpected opportunity to investigate the potentially differential impacts of fresh and old-age biomass burning on aerosol NOCs.

A high-volume air sampler (Series 2031, Laoying, China) was set up on the rooftop of a building (School of Geology and Mining Engineering, Xinjiang University). $PM_{2.5}$ samples (n = 73) were collected every five days with a duration of ~24 h onto prebaked (450 °C for ~ 10 h) quartz fiber filters (Pallflex, Pall Corporation, USA) from 1 March 2018 to 26 February 2019. One blank filter was collected every month (n = 12). All filter samples were stored at −30°C until further analysis. During the sampling campaigns, the meteorological data (e.g., temperature and relative humidity) and the concentrations of O_3 and NO_x were recorded hourly from the adjacent environmental monitoring station. These hourly data were then averaged to obtain daily values to match the sampling time of $PM_{2.5}$. In addition, the trajectories (72 h) of air masses arriving at the sampling site at each sampling event were calculated to investigate the potential influence of pollutant transport on aerosol NOCs.

157

158 **2.2. Chemical analysis**

159 A portion of each filter sample was extracted twice using 3 mL methanol (LC-MS
160 grade, CNW Technologies Ltd.) under sonication in a chilled ice slurry (~4 °C). The
161 extracted solutions were filtered through a polytetrafluoroethylene syringe filter (0.22
162 μm, CNW Technologies GmbH). Subsequently, the extracts were concentrated to 300
163 μL with a gentle stream of gaseous nitrogen (Shanghai Likang Gas Co., Ltd). The final
164 extracts were analyzed using an ultra-performance liquid chromatography quadrupole
165 time-of-flight mass spectrometry equipped with an electrospray ionization (ESI) source
166 (UPLC-ESI-QToFMS, Waters Acquity Xevo G2-XS) in both ESI+ and ESI− modes
167 (Wang et al., 2021b). It should be pointed out that UPLC-ESI-MS (i.e., TOF-only) was
168 used to identify molecular formulas of organic matter, while the functional groups of
169 the target molecule formulas were deciphered by UPLC-ESI-MS/MS (i.e., tandem mass
170 spectrometry). Ions obtained from *m/z* 50–700 were assigned molecule formulas by
171 assuming hydrogen or sodium adducts in ESI+ mode and deprotonation in ESI− mode.
172 Detailed chromatographic conditions, parameter selection, and quality control were
173 displayed in the Supplement (**Sect. S1**). Notably, there may be differences in ionization
174 efficiencies between compound types. However, the exact impacts of ionization
175 efficiency on multifunctional compounds in a complex mixture are uncertain and
176 difficult to evaluate (Ditto et al., 2022b; Yang et al., 2023). Thus, the intercomparison
177 across compound relative abundance without considering potentially differentiated
178 ionization efficiency was conducted in this study, which was similar to many previous

studies (Xu et al., 2023; Jiang et al., 2022).

For the measurement of inorganic ions, a portion of each filter sample was ultrasonically extracted with Milli-Q water (18 MΩ cm) (3 mL) in an ice-water bath (~4 °C). The extract solutions were then filtered via a polytetrafluoroethylene syringe filter (0.22 μm, Millipore, Billerica, MA). The concentrations of water-soluble inorganic ions, including NO_3^-, SO_4^{2-}, Cl^-, Ca^{2+}, Mg^{2+}, Na^+, and NH_4^+ in the samples were determined using an ion chromatograph system (Dionex Aquion, Thermo Scientific, USA) (Xu et al., 2022a; Lin et al., 2023).

2.3. Compound categorization and predictions of ALW, pH, and hydroxyl radical

The molecular formulas identified by UPLC-ESI-QToFMS were classified into several major compound classes based on their elemental compositions (i.e., C, H, O, and N), primarily including CHO, CHON, and CHN groups in the ESI+ mode and CHO, CHON, CHOS and CHONS groups in the ESI– mode (Wang et al., 2017b). CHOS and CHONS compounds were also detected in the ESI– mode, with numbers of 398 and 112, respectively (**Table S2**). As this study focused mainly on NOCs, sulfur-containing species were not discussed. Unless stated otherwise, all of the detected molecules were reported as neutral molecules. The double-bond equivalent (DBE) and carbon oxidation state (OS_C) were calculated to reflect the unsaturation degree of the organics and the composition evolution of organics that underwent oxidation processes, respectively (details in **Sect. S2**) (Kroll et al., 2011; Xu et al., 2023). The identified compounds can be further classified into four subgroups based on the number of carbon atoms and OS_C

value (Kroll et al., 2011; Xu et al., 2023). Briefly, semi-volatile oxidized organic aerosol (SV-OOA) and low-volatility oxidized organic aerosol (LV-OOA) were associated with multi-step oxidation reactions, with OS_C values between –1 and +1 and molecular formulas less than 13 carbon atoms. BBOA has OS_C values ranging from –0.5 to –1.5 and more than seven carbon atmos. Compounds with OS_C values less than –1 and carbon atoms above 20 may be related to hydrocarbon-like organic aerosol (HOA). Additionally, the modified aromaticity index (AI_{mod}) was also calculated to indicate the aromaticity of organic compounds (details in **Sect. S2**) (Koch and Dittmar, 2006). The van Krevelen diagrams and AI_{mod} values have been proposed to further classify organic matter categories (Xu et al., 2023; Su et al., 2021), according to which the identified five subgroups included saturated-like molecules (Sa, $H/C \geq 2.0$), unsaturated aliphatic-like molecules (UA, $1.5 \leq H/C < 2.0$), highly unsaturated-like molecules (HU, $AI_{mod} \leq 0.5$ and $H/C < 1.5$), highly aromatic-like molecules (HA, $0.5 < AI_{mod} \leq 0.66$), and polycyclic aromatic-like molecules (PA, $AI_{mod} > 0.66$). Furthermore, it has been suggested that the above subgroups can be subdivided into O-poor and O-rich compounds depending on their O/C ratio (**Table S8**) (Merder et al., 2020; Zhong et al., 2023).

A thermodynamic model (ISORROPIA-II) was applied to predict the mass concentration of aerosol liquid water (ALW) and the value of pH with particle-phase ion concentrations as well as ambient temperature and relative humidity as the inputs, as detailed in our previous publications (Xu et al., 2020; Xu et al., 2023; Xu et al., 2022b). The model output results based on our data set showed that 94% and 90% of

223 NO_3^- were in the aerosol phase in the cold and warm periods, respectively. Hence, the
224 predictions of pH and ALW were conducted without considering gaseous nitric acid
225 (Guo et al., 2015; Wang et al., 2021c). 78% and 21% of NH_4^+ were in the aerosol phase
226 in the cold and warm periods, respectively. Moreover, it is important to note that
227 gaseous NH_3 measurements were not conducted and ammonia partitioning was not
228 considered in this study. Thus, a bias correction of 1 pH unit was applied to calculate
229 the aerosol pH values (Guo et al., 2015; Wang et al., 2021c). The concentrations of
230 ambient •OH were predicted using empirical formula (Ehhalt and Rohrer, 2000; Wang
231 et al., 2020).
232
233 **3. Results and discussion**
234 **3.1. Overall molecular characterization of organic aerosols**
235 **Figures 1a** and **1c** show the mass spectra of organic compounds detected in ESI+
236 and ESI−, respectively. More compounds were identified in ESI+ (1885 molecular
237 formulas) than in ESI− (1091 molecular formulas) (**Table S2**), which was similar to
238 previous reports about the molecular characteristic of biomass burning aerosols and
239 urban aerosols (Jiang et al., 2022; Wang et al., 2017b). The molecular weights of the
240 compounds with relatively high signal intensity mainly ranged from 100 Da to 500 Da
241 in ESI+, which was larger than those (100–300 Da) observed in the urban (Changchun,
242 Guangzhou, and Shanghai) (Wang et al., 2021a) and agriculture (Suixi) (Wang et al.,
243 2017b) regions of China. In contrast, the species with the strong signal intensity fell
244 between 100 Da and 300 Da in ESI−. This mass range detected in Urumqi organic

aerosols was comparable to previous observations in urban (Xi'an) aerosols (Han et al., 2023) but significantly lower than that in firework-related urban (Beijing) aerosols (300–400 Da) (Xie et al., 2020). On average, the molecular number and relative abundance of CHON compounds (150–500 Da) were dominant in ESI+, accounting for 45.57% of the total molecular number and 62.70 ± 6.83% of the total signal intensity (**Figures 1a** and **Table S2**). CHO compounds were the second most abundant categories (28.76 ± 4.75% of the total signal intensity), followed by CHN compounds. However, previous observations conducted in Shanghai, Guangzhou, and Changchun suggested that the compounds in ESI+ were dominated by CHN and CHON species (Wang et al., 2021a). In ESI−, although the number of CHON compounds was less than CHO, the relative abundance of CHON compounds (150–250 Da) was higher (**Figures 1d** and **Table S2**). The finding was consistent with the results obtained in Shanghai and Changchun but different from the case in Guangzhou (Wang et al., 2021a). The average H/C ratios of CHO (1.62−1.66) and CHON (1.79−1.83) compounds in ESI+ mode (**Table S3**) were higher than those (0.94−1.13 for CHO and 1.27−1.47 for CHON) in Changchun, Shanghai, and Guangzhou (Wang et al., 2021a). However, the average O/C ratios of CHO (0.25−0.3) and CHON (0.22−0.3) compounds in ESI+ mode (**Table S3**) were less than those (0.42−0.43 for CHO and 0.27−0.45 for CHON) in the urban areas (Shanghai and Guangzhou) (Wang et al., 2021a). Overall, these dissimilarities in molecular characteristics of organic aerosols between Urumqi and other areas may be attributed to their different sources and formation mechanisms.

Figures 1b and **1d** show the time series of the fractional distributions of various organic matter categories in different ion modes. The abundance of CHO compounds in ESI+ exhibited a temporal variation similar to that of CHON compounds (r = 0.51, P < 0.01), with increased levels in the warm period. This indicated that CHO compounds may be important precursors for the formation of NOCs (via reactions in the gas- and/or particle-phases) or that they have similar origins. Previous simulation experiments have demonstrated that higher temperatures increase the concentration of oxygenated organic molecules, while lower temperatures can allow less oxidized species to condense (Stolzenburg et al., 2018; Frege et al., 2018). In addition, solar radiation and atmospheric oxidation capacity are also important factors promoting the formation of more oxygenated organic molecules (Li et al., 2022; Liu et al., 2022). Air temperature, radiation, and atmospheric oxidation capacity were much higher in the warm period than in the cold period in Urumqi (**Table S1**) (Wan et al., 2021), which may be partly responsible for increased abundances of CHO and CHON compounds in the warm period. However, the abundance of CHN compounds tended to increase from the warm period to the cold period. Since the ESI+ mode is highly sensitive to protonatable species, organic amines were expected to predominate the CHN compounds (Han et al., 2023; Wang et al., 2021a). It is well documented that the formation of amine salt in the particle phase is tightly associated with aerosol acidity and water (Liu et al., 2023). Thus, the reduced pH value and increased ALW level in the cold period (**Table S1**) provided greater potential for converting gaseous amines into particles.

In ESI− mode, the abundances of CHON and CHO compounds exhibited a significantly increased level in the cold period (**Figure 1d**), a variation pattern which was completely opposite to the case in ESI+ mode. The ESI− mode is more sensitive to deprotonatable compounds like nitrophenols, organic nitrates, organosulfates, and organic acids (Jiang et al., 2022; Lin et al., 2012). The formations of these compounds were highly impacted by ALW and aerosol acidity (Ma et al., 2021; Smith et al., 2014; Zhou et al., 2023; Xu et al., 2023). However, Urumqi has dry and dusty weather, particularly in warm period, resulting in a quite low ALW concentration (1.86 ± 1.90 μg m^{-3}) in the warm period (**Table S1**). Moreover, the calculated mean pH value was 6.86 ± 1.71 (**Table S1**) during the warm period, which implies that the fine aerosol particles in the warm period in Urumqi was neutral or slightly alkaline. Obviously, the aerosol characteristics of the warm period in Urumqi may hinder the formation of these organic compounds measured in ESI− mode. In contrast, the increased ALW concentration and decreased pH value during the cold period can facilitate the formation of CHO and CHON compounds through the partitioning of gas-phase species to the particles and subsequent aqueous phase reactions (Xu et al., 2020; Xu et al., 2023). Furthermore, the total signal intensity of CHO compounds was significantly correlated with that of CHON ($r = 0.62$, $P < 0.01$), indicating that they may have similar origins or that CHO compounds may serve as important precursors for CHON compound formation. In general, the differentiated seasonal variation patterns for the different types of NOCs measured here can be attributed to the unique meteorological conditions in Urumqi and different ionization mechanisms in ESI+ and ESI− modes. The sources

and formation mechanisms of NOCs will be further discussed in the following sections.

3.2. Seasonally differential sources and formation mechanisms of CHON compounds

CHON compounds can be derived from the reactions between CHO species and reactive nitrogen species (NO_x, NH_3, and NH_4^+) (Lee et al., 2016; De Haan et al., 2017), as also partly implied by significant positive correlations (r = 0.51–0.62, P < 0.01) between total signal intensity of CHO and CHON compounds in both ESI+ and ESI− modes. Thus, CHO compounds were further classified based on their OS_C values to preliminarily explore their origins and linkages with CHON compound formation (**Figures 2a** and **2b**). In ESI+ mode, the OS_C values of the detected CHO compounds (−1.75 to 0.5) were higher than those of primary vehicle exhausts (−2.0 to −1.9) (Aiken et al., 2008), likely indicating a weak (or indirect) contribution of primary vehicle exhausts to CHO molecules in Urumqi. The signal intensity of BBOA dominated the total OA signal intensity and was higher in the warm period than in the cold period (**Figure 2e**). However, previous studies conducted in China (e.g., Beijing, Xi'an, Shanghai, and Liaocheng) suggested that biomass burning was more significant in the cold seasons (Li et al., 2023; Wang et al., 2017a; Chen et al., 2017; Wang et al., 2009; Wang et al., 2018; Zhang et al., 2022). Furthermore, we found that the oxygen-poor unsaturated aliphatic compounds showed a high signal intensity in the warm period and that the signal intensities of all categories of compounds in the warm period were weakly correlated with atmospheric oxidants (i.e., O_3 and •OH) (r < 0.1, P > 0.05).

Thus, the formation or source of CHO compounds in the warm period may not be mainly controlled by high atmospheric oxidation but rather by biomass burning, which was distinguished from previous reports (Duan et al., 2020; Kondo et al., 2007; Zhang et al., 2023). This consideration was also supported by the fact that there were significantly more fire spots in the warm period than in the cold period (**Figure 3**). It should be noted that the materials used for biomass burning in the cold period in rural China are typically old-age plant tissues, such as dead branches of pine trees, dead branches of shrubs, corn straw, and rice straw (**Figure S3**), while biomass burning in the warm season is mainly attributed to forest fires or wildfires (relatively fresh biomass). Accordingly, a large number of fresh biomass material burning occurred from April to October each year in the neighboring countries (e.g., Kazakhstan) (Xu et al., 2021) or regions of Urumqi (due to drought) (**Figure 3**) may be largely responsible for high CHO compound abundance in the warm period.

The CHO species in ESI− had higher OS_C (–1.85 to 1.1) than those in ESI+ (–1.85 to 0.25) (**Figures 2c** and **2d**), which was consistent with a recent study conducted in Guangzhou, China (Zou et al., 2023). The predominant subgroups of CHO in ESI− were BBOA (66.4% of total signal intensity) and SV-OOA (23.1% of total signal intensity), which was different from the observation in Shanghai (dominated by SV-OOA and LV-OOA) (Wang et al., 2017a). Additionally, some specific saturated and unsaturated aliphatic CHO substances (i.e., $C_{12–18}H_nO_2$) in ESI− showed higher abundance in the warm season than in the cold season, which was contrary to the variation pattern of other CHO compounds. These $C_{12–18}H_nO_2$ compounds were found

355 to be mainly fatty acids, such as stearic acid ($C_{18}H_{36}O_2$), oleic acid ($C_{18}H_{34}O_2$),
356 linolelaidic acid ($C_{18}H_{32}O_2$), palmitic acid ($C_{16}H_{32}O_2$), and palmitoleic acid ($C_{16}H_{30}O_2$)
357 (**Figure S4**), all of which usually accumulate in plants, particularly *Suaeda*
358 *aralocaspica* (W. Hogg and T. Gillan, 1984; Wang et al., 2011). Interestingly, this plant
359 was widely distributed in Central Asia as well as on the southern edge of the Junggar
360 Basin in Xinjiang, China (Wang et al., 2011). Although fatty acids can also originate
361 from food cooking (Zhao et al., 2007), there seem to be no seasonal differences in
362 cooking behavior locally. Thus, these results further confirmed our consideration that
363 the abundance of CHO compounds in the warm period was highly impacted by fresh
364 biomass material burning (e.g., forest fires or wildfires).

365 CHON molecules in ESI+ were mainly identified as unsaturated aliphatic-like
366 compounds that are oxygen poor (**Figures 4a** and **4b**), accounting for more than 70%
367 of the total signal intensities of CHON species (**Figure S5**). The signal intensity of
368 CHON species in ESI+ was greater in the warm period than in the cold period (**Figure**
369 **4e**). Moreover, BBOA contributed to 56.9 % of the total CHON signal intensity in the
370 warm period (**Figure S6**). These characteristics of CHON compounds were similar to
371 those of CHO. Considering a significant positive correlation (r = 0.62, P < 0.01)
372 between the total signal intensity of CHO and CHON compounds in ESI+, we thus
373 concluded that primary sources (i.e., fresh biomass material burning) were also one of
374 the main sources of CHON compounds. In this study, CHON compounds with O/N <
375 3 contributed 76.48 ± 1.11% of total CHON species in ESI+ (**Figure S7**), which was
376 much larger than the results observed in urban Tianjin in winter (less than 20%) (Zhong

et al., 2023). In particular, $C_{16}H_{33}ON$, $C_{18}H_{37}ON$, $C_{18}H_{35}ON$, $C_{18}H_{33}ON$, $C_{18}H_{31}ON$, and $C_{20}H_{33}ON$ showed a high abundance, together accounting for 55.04 ± 7.09 % of the total CHON abundance (**Table S4**). The carbon number of these compounds was consistent with that of fatty acids mentioned above; moreover, their abundances showed a positive correlation (r = 0.43–0.81, $P < 0.01$) with the abundances of corresponding fatty acids in the warm period. In contrast, these CHON compounds only showed a weak correlation ($r = -0.24 \sim 0.33$) with atmospheric oxidants (e.g., •OH, O_3, and NO_x). Thus, the formation mechanism of biomass burning-related NOCs in Urumqi during the warm period may be the interaction between fatty acids and reduced nitrogen species (e.g., NH_3) rather than the oxidation pathway involving CHO compounds and NO_x.

A recent laboratory study has suggested that NH_3 produced during the thermal degradation of amino acids can react with oleic acid from the pyrolysis of triglycerides to form amides (R1) (Ditto et al., 2022a). As discussed above, the combustion of fresh biomass materials (e.g., forest fires or wildfires) can release abundant fatty acids. In addition, wildfires can also emit large amounts of NH_3, with an average emission factor more than twice the NH_3 emission factor of agricultural fires (Tomsche et al., 2023). According to MS/MS analysis (**Table S5**), potential fatty acid-derived NOCs were indeed identified as amides. Thus, we proposed that the high temperature generated during wildfires or forest fires provides suitable conditions for the reaction of carboxylic acids and NH_3 to form amides. The specific process was presented in **Figure 5** (Pathway 1). It has been suggested that atmospheric oxidants can oxidize olefins (R2

and R3) to form hydroxyl nitrates and carbonyl nitrates (Perring et al., 2013). Therefore, fatty acids (oleic acid as a representative) released from fresh biomass material burning may also rely on oxidation pathways to form NOCs (**Figure 5**, Pathway 2). It is worth noting that some products with double bonds after the amidation of unsaturated fatty acids can continue to undergo the reactions of R2 and R3 in the atmosphere, resulting in the formation of nitrooxy amides (**Figure 5**, Pathway 3). However, we found that the abundance of oleic acid-derived amides via Pathway 1 in the warm period was more than 100 times higher than that of NOCs with $–ONH_2$ (thus, the impact of ionization efficiency is expected to be less than 100 times) from Pathways 3. In the cold period, the abundance of fatty acids-derived amides decreased dramatically (**Figure 5** and **Figure S8**). Thus, the overall results demonstrated that the combustion of fresh biomass materials indeed contributed significantly to aerosol NOCs (e.g., amides) in the warm period in Urumqi.

$$ROOH \xrightarrow[-H_2O \text{ and high temperature}]{NH_3} RCONH_2 \quad (R1)$$

$$RH \xrightarrow{\bullet OH} R\bullet \xrightarrow{O_2} RO_2\bullet \xrightarrow{NO} RONO_2 \quad (R2)$$

$$R_1{=}R_2 \xrightarrow{NO_3\bullet} R_1(ONO_2)\text{-}R_2\bullet \xrightarrow{O_2} R_1(ONO_2)\text{-}R_2O_2\bullet \xrightarrow{RO_2\bullet,\ NO_3\bullet} R_1(ONO_2)\text{-}R_2(O) \quad (R3)$$

The CHON species detected in ESI− were mainly aromatic-like compounds, whose signal intensities were significantly greater in the cold period than in the warm period (**Figures 4c,4e** and **Figure S5**). Moreover, we found that several nitro-aromatic compounds, including $C_6H_5O_3N$, $C_6H_5O_4N$, $C_7H_7O_3N$, $C_7H_7O_4N$, $C_7H_5O_5N$, and $C_8H_9O_3N$ (confirmed by their authentic standards in the LC/MS analysis), contributed

up to 50% of the total CHON (ESI− mode) intensity (**Table S6**). Other NOCs with relatively high signal intensity were mainly $O_{4\text{-}6}N_2$ species (contributed up to 25%), such as $C_6H_4O_5N_2$, $C_7H_4O_7N_2$, $C_7H_6O_5N_2$, and $C_7H_6O_6N_2$, which have been suggested to be associated with secondary photochemical or multiphase chemical processes (Harrison et al., 2005; Cecinato et al., 2005; Salvador et al., 2021). However, the abovementioned nitro-aromatic compounds including $C_6H_5O_3N$ (nitrophenol), $C_6H_5O_4N$ (nitrocatechol), $C_7H_7O_3N$ (methyl-nitrophenol), and $C_7H_7O_4N$ (methyl-nitrocatechol) were primarily identified as tracers of straw and wood burning (old-age biomass materials commonly used in suburban and rural China) (Iinuma et al., 2010; Kourtchev et al., 2016). A study about molecular characterization (ESI− mode) of water-soluble aerosols emitted from the combustion of old-age biomass materials (i.e., dry corn straw, rice straw, and pine branches) and coal showed that OA from old-age biomass burning typically contained much more nitro compounds and/or organonitrates than that from coal, while OA from coal-smoke contained more sulfur-containing compounds (Song et al., 2018). Thus, the old-age biomass burning associated with winter heating rather than coal combustion may contribute a significant amount of aerosol NOCs (e.g., nitrophenols) in wintertime Urumqi. However, it does not necessarily suggest that the importance of multiphase chemistry in the formation of NOCs was ignorable, as indicated by relatively high signal intensity of $O_{4\text{-}6}N_2$ species. In general, the differential molecular characteristics of CHON species in different seasons in Urumqi can largely attributed to different impacts of the combustion of fresh- and old-age biomass materials.

3.3. CHN molecule evidence of fresh and old-age biomass burning in different periods.

Figures 6a and **6b** present the van Krevelen diagram of CHN compounds in the cold and warm periods. The CHN_1 compounds with relatively high signal intensity mainly contained 7–20 carbon atoms, among which $C_5H_5N(CH_2)_n$, $C_9H_7N(CH_2)_n$, and $C_{13}H_9N(CH_2)_n$ were dominant (78.68 ± 7.59 % of the total signal intensity of CHN_1 compounds in the cold period, **Table S7**). $C_5H_5N(CH_2)_n$ could be identified as pyridine and its homologues, which have been detected in freshly discharged BBOA (Dou et al., 2015). Additionally, the abundance of $C_5H_5N(CH_2)_n$ was positively correlated with that of $C_9H_7N(CH_2)_n$, $C_{13}H_9N(CH_2)_n$, and nitro-aromatic compounds mentioned above (r = 0.46−0.81, $P < 0.01$), particularly in the cold period with old-age biomass burning for heating. We further found that both the total signal intensity and aromaticity of CHN_1 species were much higher in the cold period (AI_{mod} of 0.52) than in the warm period (AI_{mod} of 0.35) (**Figure 6** and **Figure S9**). It has been suggested that old-age leaves contain more aromatic compounds compared to fresh leaves (Jian et al., 2016). Thus, the overall results implied that old-age biomass burning had an important contribution to the variation of CHN_1 compounds. In particular, the intensity of CHN_1 compounds was significantly negatively correlated with the concentration of O_3 and ·OH (r = −0.44 ~ −0.53, $P < 0.01$), suggesting that atmospheric oxidation processes were the potential pathway for amine removal rather than the sources of particle amine salts (Zahardis et al., 2008; Qiu and Zhang, 2013). This result differed from the previous case, which

showed that the formation processes of CHN_1 and its homologs in Guangzhou (South China) were tightly related to photo-oxidation processes (Jiang et al., 2022). The CHN_2 species showed a similar temporal variation pattern to the CHN_1 species. Moreover, the abundances of total CHN_2 and major components ($C_{8\text{-}11}H_8N_2(CH_2)_n$, $C_{10}H_{14}N_2(CH_2)_n$, $C_{10}H_{16}N_2(CH_2)_n$ and $C_5H_8N_2(CH_2)_n$) were positively correlated with that of total CHN_1 (r = 0.55−0.90, P < 0.01), but negatively correlated with the concentration of O_3 and ·OH (r = −0.43 ~ −0.60, P < 0.01). Clearly, old-age biomass burning, particularly in the cold period, also exerted significant impacts on the abundance of CHN_2 compounds, which was also supported by several previous studies (Laskin et al., 2009; Wang et al., 2017b; Song et al., 2022). A study about molecular characterization (ESI+ mode) of humic-like substances emitted from the combustion of old-age biomass materials (i.e., dry corn straw, rice straw, and pine branches) and coals showed that OA from old-age biomass burning typically contained much more CHN_2 compounds (55–64%) than that from coal (20–37%), while OA from coal-smoke showed more CHN_1 compounds (78–84%) compared to that from old-age biomass materials (15–22%) (Song et al., 2022). In this study, the signal intensity of CHN_1 compounds in the cold period was about 40% higher than that in the warm period, while that of CHN_2 compounds showed a 160% increase from the warm period to the cold period. Thus, although the contribution of fossil fuel (e.g., coal) combustion to NOCs in the cold period cannot be ignored, our results at least suggested that the biomass burning-derived CHN compounds showed a more significant increase compared to coal combustion-derived compounds from the warm period to the cold period in Urumqi.

Interestingly, we found some CHN species with 16–20 carbon atoms showed higher abundance in the warm period than in the cold period, a pattern opposite to that of all other CNH compounds (**Figure 6c**). These $C_{16–20}N_1H_x$ compounds were further identified as alkyl nitriles (**Table S5**) (Simoneit et al., 2003). In addition, the carbon number of the identified alkyl nitriles was consistent with those of amides previously proposed to be produced by fresh biomass burning. Thus, we proposed that fresh biomass material burning in the warm period may provide a continuous high-temperature environment to promote the dehydration of amides (**Figure 5**, Pathway 4). These alkyl nitriles with double bonds can continue to undergo the reactions of R2 and R3 **(Figure 5**, Pathway 5**)**. However, the signal intensity of the nitrooxy products in the warm period was insignificantly correlated with the concentration of O_3, ·OH, and NO_x ($P > 0.05$), likely indicating a weak influence of atmospheric oxidation on alkyl nitrile removal in this site. The high-temperature dehydration of amides (e.g., erucamide) to form alkyl nitriles (e.g., erucyl nitrile) has been demonstrated by Simoneit et al. (2003) in a laboratory simulation experiment. A study on BBOA also showed that alkyl nitriles can be serve as indicators of biomass burning in the ambient atmosphere (Radzi Bin Abas et al., 2004). Furthermore, the abundance of identified alkyl nitriles initially increased from March and peaked in September and October (**Figure S10**), a pattern which was consistent with the interannual variation in wildfire areas (more in the warm period) in Central Asian countries (Xu et al., 2021). Although cooking is also a potential source of alkyl nitriles (Schauer et al., 1999), this activity does not have seasonal differences. In contrast, the dramatically increased abundance of aromatic CNH

compounds in the cold period (**Figure S9**) can be attributed to the aqueous reactions of amines emitted from old-age biomass material and coal combustion with acidic substances, as indicated by significant correlations (r = 0.61−0.95, P < 0.01) between total CHN abundance and SO_4^{2-} and NO_3^- concentrations. These findings further confirmed that the NOCs from the combustion of fresh biomass materials in the warm period in suburban Urumqi were compositionally different from those from old-age biomass burning in the cold period.

4. Conclusions

The complexity of NOCs restricts our understanding of its sources and formation processes. In this study, the molecular compositions of organic aerosols in $PM_{2.5}$ collected in Urumqi over a one-year period were systematically characterized in both ESI− and ESI+ modes, with a major focus on NOCs. A large amount of NOCs were identified, showing that NOCs in relatively highly oxidative and reduced forms can be roughly distinguished via these two ionization modes. Based on the identification of molecular markers of amides and alkyl nitriles (much higher in the warm period) and the analysis of their formation mechanisms (less contribution of atmospheric oxidation), we highlighted the important contribution of combustion of fresh biomass materials such as forest fires and wildfires to NOCs in the warm season in Urumqi. In contrast, the dramatically increased abundances of aromatic CNH compounds and nitro-aromatic CHON compounds (mainly nitrophenols) in the cold period were tightly associated with the impacts of old-age biomass material burning. These results were illustrated in

a diagram (**Figure 7**).

Biomass materials in rural China were typically old-age plant tissues, as mentioned above. Fresh biomass materials (e.g., green vegetation) with the enrichment of oils and proteins can exist in forest fires or wildfires. Indeed, previous studies have suggested that biomass burning can lead to the formation of aerosol amines and nitriles. However, field observation studies have yet to pay attention to the differences in aerosol NOCs emitted from the combustion of fresh and old-age biomass materials. For the first time, our results reveal that fresh biomass material combustion can contribute more amines and nitriles than old-age biomass material combustion. Generally, this study provides field evidence on the differential impacts of the combustion of fresh and old-age biomass materials on aerosol NOCs, improving our current understanding of the molecular compositions of organic nitrogen aerosols in a vast territory with a sparse population in Northwest China. Moreover, according to the fact that the studied site is highly affected by combustion emissions of different types of biomass materials, future work is needed to deeply understand the quantitative contributions of different types of biomass burning to OA in China.

Data availability. The data in this study are available at https://doi.org/10.5281/zenodo.10453929

Competing interests. The authors declare no conflicts of interest relevant to this study.

Supplement. Details of chemical analysis and data processing, eight tables (Tables S1−S8), and ten extensive figures (Figures S1−S10).

Author contributions. YX designed the study. YJM, TY, and HWX performed field measurements and sample collection; YJM and TY performed chemical analysis; YX and YJM performed data analysis; YX and YJM wrote the original manuscript; and YX, YJM, HWX, and HYX reviewed and edited the manuscript.

Financial support. This study was kindly supported by the National Natural Science Foundation of China through grant 42303081 (Y. Xu) and Shanghai "Science and Technology Innovation Action Plan" Shanghai Sailing Program through grant 22YF1418700 (Y. Xu).

References

Aiken, A. C., Decarlo, P. F., Kroll, J. H., Worsnop, D. R., Huffman, J. A., Docherty, K. S., Ulbrich, I. M., Mohr, C., Kimmel, J. R., Sueper, D., Sun, Y., Zhang, Q., Trimborn, A., Northway, M., Ziemann, P. J., Canagaratna, M. R., Onasch, T. B., Alfarra, M. R., Prevot, A. S., Dommen, J., Duplissy, J., Metzger, A., Baltensperger, U., and Jimenez, J. L.: O/C and OM/OC ratios of primary, secondary, and ambient organic aerosols with high-resolution time-of-flight aerosol mass spectrometry, Environ. Sci. Technol., 42, 4478-4485, https://doi.org/10.1021/es703009q, 2008.

Altieri, K. E., Fawcett, S. E., Peters, A. J., Sigman, D. M., and Hastings, M. G.:

574 Marine biogenic source of atmospheric organic nitrogen in the subtropical North
575 Atlantic, P. Natl. Acad. Sci. USA, 113, 925-930,
576 https://doi.org/10.1073/pnas.1516847113, 2016.
577 Bandowe, B. A. M. and Meusel, H.: Nitrated polycyclic aromatic hydrocarbons
578 (nitro-PAHs) in the environment – A review, Sci. Total Environ., 581-582, 237-257,
579 https://doi.org/10.1016/j.scitotenv.2016.12.115, 2017.
580 Bátori, Z., Erdős, L., Kelemen, A., Deák, B., Valkó, O., Gallé, R., Bragina, T. M.,
581 Kiss, P. J., Kröel-Dulay, G., and Tölgyesi, C.: Diversity patterns in sandy forest-steppes:
582 a comparative study from the western and central Palaearctic, Biodivers. Conserv., 27,
583 1011-1030, https://doi.org/10.1007/s10531-017-1477-7, 2018.
584 Cape, J. N., Cornell, S. E., Jickells, T. D., and Nemitz, E.: Organic nitrogen in the
585 atmosphere — Where does it come from? A review of sources and methods, Atmos.
586 Res., 102, 30-48, https://doi.org/10.1016/j.atmosres.2011.07.009, 2011.
587 Cecinato, A., Di Palo, V., Pomata, D., Tomasi Scianò, M. C., and Possanzini, M.:
588 Measurement of phase-distributed nitrophenols in Rome ambient air, Chemosphere, 59,
589 679-683, https://doi.org/10.1016/j.chemosphere.2004.10.045, 2005.
590 Chen, J., Li, C., Ristovski, Z., Milic, A., Gu, Y., Islam, M. S., Wang, S., Hao, J.,
591 Zhang, H., He, C., Guo, H., Fu, H., Miljevic, B., Morawska, L., Thai, P., Lam, Y. F.,
592 Pereira, G., Ding, A., Huang, X., and Dumka, U. C.: A review of biomass burning:
593 Emissions and impacts on air quality, health and climate in China, Sci. Total Environ.,
594 579, 1000-1034, https://doi.org/10.1016/j.scitotenv.2016.11.025, 2017.
595 De Haan, D. O., Hawkins, L. N., Welsh, H. G., Pednekar, R., Casar, J. R.,

Pennington, E. A., de Loera, A., Jimenez, N. G., Symons, M. A., Zauscher, M., Pajunoja, A., Caponi, L., Cazaunau, M., Formenti, P., Gratien, A., Pangui, E., and Doussin, J.-F.: Brown Carbon Production in Ammonium- or Amine-Containing Aerosol Particles by Reactive Uptake of Methylglyoxal and Photolytic Cloud Cycling, Environ. Sci. Technol., 51, 7458-7466, https://doi.org/10.1021/acs.est.7b00159, 2017.

Ditto, J. C., Abbatt, J. P. D., and Chan, A. W. H.: Gas- and Particle-Phase Amide Emissions from Cooking: Mechanisms and Air Quality Impacts, Environ. Sci. Technol., 56, 7741-7750, https://doi.org/10.1021/acs.est.2c01409, 2022a.

Ditto, J. C., Machesky, J., and Gentner, D. R.: Analysis of reduced and oxidized nitrogen-containing organic compounds at a coastal site in summer and winter, Atmos. Chem. Phys., 22, 3045-3065, https://doi.org/10.5194/acp-22-3045-2022, 2022b.

Ditto, J. C., Joo, T., Slade, J. H., Shepson, P. B., Ng, N. L., and Gentner, D. R.: Nontargeted Tandem Mass Spectrometry Analysis Reveals Diversity and Variability in Aerosol Functional Groups across Multiple Sites, Seasons, and Times of Day, Environ. Sci. Technol. Lett., 7, 60-69, https://doi.org/10.1021/acs.estlett.9b00702, 2020.

Dou, J., Lin, P., Kuang, B.-Y., and Yu, J. Z.: Reactive Oxygen Species Production Mediated by Humic-like Substances in Atmospheric Aerosols: Enhancement Effects by Pyridine, Imidazole, and Their Derivatives, Environ. Sci. Technol., 49, 6457-6465, https://doi.org/10.1021/es5059378, 2015.

Duan, J., Huang, R. J., Li, Y., Chen, Q., Zheng, Y., Chen, Y., Lin, C., Ni, H., Wang, M., Ovadnevaite, J., Ceburnis, D., Chen, C., Worsnop, D. R., Hoffmann, T., O'Dowd, C., and Cao, J.: Summertime and wintertime atmospheric processes of secondary

618 aerosol in Beijing, Atmos. Chem. Phys., 20, 3793-3807, https://doi.org/10.5194/acp-
619 20-3793-2020, 2020.
620 Ehhalt, D. H. and Rohrer, F.: Dependence of the OH concentration on solar UV, J.
621 Geophys. Res.-Atmos., 105, 3565-3571, https://doi.org/10.1029/1999JD901070, 2000.
622 Franze, T., Weller, M. G., Niessner, R., and Pöschl, U.: Protein Nitration by
623 Polluted Air, Environ. Sci. Technol., 39, 1673-1678, https://doi.org/10.1021/es0488737,
624 2005.
625 Frege, C., Ortega, I. K., Rissanen, M. P., Praplan, A. P., Steiner, G., Heinritzi, M.,
626 Ahonen, L., Amorim, A., Bernhammer, A. K., Bianchi, F., Brilke, S., Breitenlechner,
627 M., Dada, L., Dias, A., Duplissy, J., Ehrhart, S., El-Haddad, I., Fischer, L., Fuchs, C.,
628 Garmash, O., Gonin, M., Hansel, A., Hoyle, C. R., Jokinen, T., Junninen, H., Kirkby, J.,
629 Kürten, A., Lehtipalo, K., Leiminger, M., Mauldin, R. L., Molteni, U., Nichman, L.,
630 Petäjä, T., Sarnela, N., Schobesberger, S., Simon, M., Sipilä, M., Stolzenburg, D., Tomé,
631 A., Vogel, A. L., Wagner, A. C., Wagner, R., Xiao, M., Yan, C., Ye, P., Curtius, J.,
632 Donahue, N. M., Flagan, R. C., Kulmala, M., Worsnop, D. R., Winkler, P. M., Dommen,
633 J., and Baltensperger, U.: Influence of temperature on the molecular composition of
634 ions and charged clusters during pure biogenic nucleation, Atmos. Chem. Phys., 18, 65-
635 79, https://doi.org/10.5194/acp-18-65-2018, 2018.
636 Guo, H., Xu, L., Bougiatioti, A., Cerully, K. M., Capps, S. L., Hite Jr, J. R., Carlton,
637 A. G., Lee, S. H., Bergin, M. H., Ng, N. L., Nenes, A., and Weber, R. J.: Fine-particle
638 water and pH in the southeastern United States, Atmos. Chem. Phys., 15, 5211-5228,
639 https://doi.org/10.5194/acp-15-5211-2015, 2015.

Han, Y., Zhang, X., Li, L., Lin, Y., Zhu, C., Zhang, N., Wang, Q., and Cao, J.: Enhanced Production of Organosulfur Species during a Severe Winter Haze Episode in the Guanzhong Basin of Northwest China, Environ. Sci. Technol., https://doi.org/10.1021/acs.est.3c02914, 2023.

Harrison, M. A. J., Barra, S., Borghesi, D., Vione, D., Arsene, C., and Iulian Olariu, R.: Nitrated phenols in the atmosphere: a review, Atmos. Environ., 39, 231-248, https://doi.org/10.1016/j.atmosenv.2004.09.044, 2005.

Iinuma, Y., Böge, O., Gräfe, R., and Herrmann, H.: Methyl-Nitrocatechols: Atmospheric Tracer Compounds for Biomass Burning Secondary Organic Aerosols, Environ. Sci. Technol., 44, 8453-8459, https://doi.org/10.1021/es102938a, 2010.

Jian, Q., Boyer, T. H., Yang, X., Xia, B., and Yang, X.: Characteristics and DBP formation of dissolved organic matter from leachates of fresh and aged leaf litter, Chemosphere, 152, 335-344, https://doi.org/10.1016/j.chemosphere.2016.02.107, 2016.

Jiang, H., Li, J., Tang, J., Zhao, S., Chen, Y., Tian, C., Zhang, X., Jiang, B., Liao, Y., and Zhang, G.: Factors Influencing the Molecular Compositions and Distributions of Atmospheric Nitrogen-Containing Compounds, J. Geophys. Res.-Atmos., 127, e2021JD036284, https://doi.org/10.1029/2021JD036284, 2022.

Kenagy, H. S., Romer Present, P. S., Wooldridge, P. J., Nault, B. A., Campuzano-Jost, P., Day, D. A., Jimenez, J. L., Zare, A., Pye, H. O. T., Yu, J., Song, C. H., Blake, D. R., Woo, J.-H., Kim, Y., and Cohen, R. C.: Contribution of Organic Nitrates to Organic Aerosol over South Korea during KORUS-AQ, Environ. Sci. Technol., 55, 16326-16338, https://doi.org/10.1021/acs.est.1c05521, 2021.

662 Koch, B. P. and Dittmar, T.: From mass to structure: an aromaticity index for high-
663 resolution mass data of natural organic matter, Rapid Commun. Mass Spectrom., 20,
664 926-932, https://doi.org/10.1002/rcm.2386, 2006.
665 Kondo, Y., Miyazaki, Y., Takegawa, N., Miyakawa, T., Weber, R. J., Jimenez, J.
666 L., Zhang, Q., and Worsnop, D. R.: Oxygenated and water-soluble organic aerosols in
667 Tokyo, J. Geophys. Res.-Atmos., 112, https://doi.org/10.1029/2006JD007056, 2007.
668 Kourtchev, I., Godoi, R. H. M., Connors, S., Levine, J. G., Archibald, A. T., Godoi,
669 A. F. L., Paralovo, S. L., Barbosa, C. G. G., Souza, R. A. F., Manzi, A. O., Seco, R.,
670 Sjostedt, S., Park, J. H., Guenther, A., Kim, S., Smith, J., Martin, S. T., and Kalberer,
671 M.: Molecular composition of organic aerosols in central Amazonia: an ultra-high-
672 resolution mass spectrometry study, Atmos. Chem. Phys., 16, 11899-11913,
673 https://doi.org/10.5194/acp-16-11899-2016, 2016.
674 Kroll, J. H., Donahue, N. M., Jimenez, J. L., Kessler, S. H., Canagaratna, M. R.,
675 Wilson, K. R., Altieri, K. E., Mazzoleni, L. R., Wozniak, A. S., Bluhm, H., Mysak, E.
676 R., Smith, J. D., Kolb, C. E., and Worsnop, D. R.: Carbon oxidation state as a metric
677 for describing the chemistry of atmospheric organic aerosol, Nat. Chem., 3, 133-139,
678 https://doi.org/10.1038/nchem.948, 2011.
679 Laskin, A., Smith, J. S., and Laskin, J.: Molecular Characterization of Nitrogen-
680 Containing Organic Compounds in Biomass Burning Aerosols Using High-Resolution
681 Mass Spectrometry, Environ. Sci. Technol., 43, 3764-3771,
682 https://doi.org/10.1021/es803456n, 2009.
683 Laskin, J., Laskin, A., Nizkorodov, S. A., Roach, P., Eckert, P., Gilles, M. K., Wang,

B., Lee, H. J., and Hu, Q.: Molecular Selectivity of Brown Carbon Chromophores, Environ. Sci. Technol., 48, 12047-12055, https://doi.org/10.1021/es503432r, 2014.

Lee, B. H., Mohr, C., Lopez-Hilfiker, F. D., Lutz, A., Hallquist, M., Lee, L., Romer, P., Cohen, R. C., Iyer, S., Kurtén, T., Hu, W., Day, D. A., Campuzano-Jost, P., Jimenez, J. L., Xu, L., Ng, N. L., Guo, H., Weber, R. J., Wild, R. J., Brown, S. S., Koss, A., de Gouw, J., Olson, K., Goldstein, A. H., Seco, R., Kim, S., McAvey, K., Shepson, P. B., Starn, T., Baumann, K., Edgerton, E. S., Liu, J., Shilling, J. E., Miller, D. O., Brune, W., Schobesberger, S., D'Ambro, E. L., and Thornton, J. A.: Highly functionalized organic nitrates in the southeast United States: Contribution to secondary organic aerosol and reactive nitrogen budgets, P. Natl. Acad. Sci. USA, 113, 1516-1521, https://doi.org/10.1073/pnas.1508108113, 2016.

Li, S., Liu, D., Kong, S., Wu, Y., Hu, K., Zheng, H., Cheng, Y., Zheng, S., Jiang, X., Ding, S., Hu, D., Liu, Q., Tian, P., Zhao, D., and Sheng, J.: Evolution of source attributed organic aerosols and gases in a megacity of central China, Atmos. Chem. Phys., 22, 6937-6951, https://doi.org/10.5194/acp-22-6937-2022, 2022.

Li, Y., Chen, M., Wang, Y., Huang, T., Wang, G., Li, Z., Li, J., Meng, J., and Hou, Z.: Seasonal characteristics and provenance of organic aerosols in the urban atmosphere of Liaocheng in the North China Plain: Significant effect of biomass burning, Particuology, 75, 185-198, https://doi.org/10.1016/j.partic.2022.07.012, 2023.

Lin, P., Rincon, A. G., Kalberer, M., and Yu, J. Z.: Elemental Composition of HULIS in the Pearl River Delta Region, China: Results Inferred from Positive and Negative Electrospray High Resolution Mass Spectrometric Data, Environ. Sci.

706 Technol., 46, 7454-7462, https://doi.org/10.1021/es300285d, 2012.

707 Lin, X., Xu, Y., Zhu, R.-G., Xiao, H.-W., and Xiao, H.-Y.: Proteinaceous Matter in
708 $PM_{2.5}$ in Suburban Guiyang, Southwestern China: Decreased Importance in Long-
709 Range Transport and Atmospheric Degradation, J. Geophys. Res.-Atmos., 128,
710 e2023JD038516, https://doi.org/10.1029/2023JD038516, 2023.

711 Liu, T., Xu, Y., Sun, Q.-B., Xiao, H.-W., Zhu, R.-G., Li, C.-X., Li, Z.-Y., Zhang,
712 K.-Q., Sun, C.-X., and Xiao, H.-Y.: Characteristics, Origins, and Atmospheric
713 Processes of Amines in Fine Aerosol Particles in Winter in China, J. Geophys. Res.-
714 Atmos., 128, e2023JD038974, https://doi.org/10.1029/2023JD038974, 2023.

715 Liu, T., Hong, Y., Li, M., Xu, L., Chen, J., Bian, Y., Yang, C., Dan, Y., Zhang, Y.,
716 Xue, L., Zhao, M., Huang, Z., and Wang, H.: Atmospheric oxidation capacity and ozone
717 pollution mechanism in a coastal city of southeastern China: analysis of a typical
718 photochemical episode by an observation-based model, Atmos. Chem. Phys., 22, 2173-
719 2190, https://doi.org/10.5194/acp-22-2173-2022, 2022.

720 Ma, L., Guzman, C., Niedek, C., Tran, T., Zhang, Q., and Anastasio, C.: Kinetics
721 and Mass Yields of Aqueous Secondary Organic Aerosol from Highly Substituted
722 Phenols Reacting with a Triplet Excited State, Environ. Sci. Technol., 55, 5772-5781,
723 https://doi.org/10.1021/acs.est.1c00575, 2021.

724 Merder, J., Freund, J. A., Feudel, U., Hansen, C. T., Hawkes, J. A., Jacob, B.,
725 Klaproth, K., Niggemann, J., Noriega-Ortega, B. E., Osterholz, H., Rossel, P. E., Seidel,
726 M., Singer, G., Stubbins, A., Waska, H., and Dittmar, T.: ICBM-OCEAN: Processing
727 Ultrahigh-Resolution Mass Spectrometry Data of Complex Molecular Mixtures, Anal.

728 Chem., 92, 6832-6838, https://dx.doi.org/10.1021/acs.analchem.9b05659, 2020.
729 Nguyen, T. B., Bates, K. H., Crounse, J. D., Schwantes, R. H., Zhang, X.,
730 Kjaergaard, H. G., Surratt, J. D., Lin, P., Laskin, A., Seinfeld, J. H., and Wennberg, P.
731 O.: Mechanism of the hydroxyl radical oxidation of methacryloyl peroxynitrate (MPAN)
732 and its pathway toward secondary organic aerosol formation in the atmosphere, Phys.
733 Chem. Chem. Phys., 17, 17914-17926, https://doi.org/10.1039/C5CP02001H, 2015.
734 Perring, A. E., Pusede, S. E., and Cohen, R. C.: An Observational Perspective on
735 the Atmospheric Impacts of Alkyl and Multifunctional Nitrates on Ozone and
736 Secondary Organic Aerosol, Chem. Rev., 113, 5848-5870,
737 https://doi.org/10.1021/cr300520x, 2013.
738 Qiu, C. and Zhang, R.: Multiphase chemistry of atmospheric amines, Phys. Chem.
739 Chem. Phys., 15, 5738-5752, https://doi.org/10.1039/C3CP43446j, 2013.
740 Qizhi, M., Ying, L., Kang, W., and Qingfei, Z.: Spatio-Temporal Changes of
741 Population Density and Urbanization Pattern in China(2000–2010), China City Plan.
742 Rev., 25, 8-14, 2016.
743 Radzi Bin Abas, M., Rahman, N. A., Omar, N. Y. M. J., Maah, M. J., Abu Samah,
744 A., Oros, D. R., Otto, A., and Simoneit, B. R. T.: Organic composition of aerosol
745 particulate matter during a haze episode in Kuala Lumpur, Malaysia, Atmos. Environ.,
746 38, 4223-4241, https://doi.org/10.1016/j.atmosenv.2004.01.048, 2004.
747 Ren, Y., Wang, G., Wu, C., Wang, J., Li, J., Zhang, L., Han, Y., Liu, L., Cao, C.,
748 Cao, J., He, Q., and Liu, X.: Changes in concentration, composition and source
749 contribution of atmospheric organic aerosols by shifting coal to natural gas in Urumqi,

Atmos. Environ., 148, 306-315, https://doi.org/10.1016/j.atmosenv.2016.10.053, 2017.

Rollins, A. W., Browne, E. C., Min, K.-E., Pusede, S. E., Wooldridge, P. J., Gentner, D. R., Goldstein, A. H., Liu, S., Day, D. A., Russell, L. M., and Cohen, R. C.: Evidence for NO_x Control over Nighttime SOA Formation, Science, 337, 1210-1212, https://doi.org/10.1126/science.1221520, 2012.

Salvador, C. M. G., Tang, R., Priestley, M., Li, L., Tsiligiannis, E., Le Breton, M., Zhu, W., Zeng, L., Wang, H., Yu, Y., Hu, M., Guo, S., and Hallquist, M.: Ambient nitro-aromatic compounds – biomass burning versus secondary formation in rural China, Atmos. Chem. Phys., 21, 1389-1406, https://doi.org/10.5194/acp-21-1389-2021, 2021.

Samy, S. and Hays, M. D.: Quantitative LC–MS for water-soluble heterocyclic amines in fine aerosols ($PM_{2.5}$) at Duke Forest, USA, Atmos. Environ., 72, 77-80, https://doi.org/10.1016/j.atmosenv.2013.02.032, 2013.

Schauer, J. J., Kleeman, M. J., Cass, G. R., and Simoneit, B. R. T.: Measurement of Emissions from Air Pollution Sources. 1. C_1 through C_{29} Organic Compounds from Meat Charbroiling, Environ. Sci. Technol., 33, 1566-1577, https://doi.org/10.1021/es980076j, 1999.

Seinfeld, J. H., Bretherton, C., Carslaw, K. S., Coe, H., DeMott, P. J., Dunlea, E. J., Feingold, G., Ghan, S., Guenther, A. B., Kahn, R., Kraucunas, I., Kreidenweis, S. M., Molina, M. J., Nenes, A., Penner, J. E., Prather, K. A., Ramanathan, V., Ramaswamy, V., Rasch, P. J., Ravishankara, A. R., Rosenfeld, D., Stephens, G., and Wood, R.: Improving our fundamental understanding of the role of aerosol−cloud interactions in the climate system, P. Natl. Acad. Sci. USA, 113, 5781-5790,

https://doi.org/10.1073/pnas.1514043113, 2016.

Simoneit, B. R. T., Rushdi, A. I., bin Abas, M. R., and Didyk, B. M.: Alkyl Amides and Nitriles as Novel Tracers for Biomass Burning, Environ. Sci. Technol., 37, 16-21, https://doi.org/10.1021/es020811y, 2003.

Smith, J. D., Sio, V., Yu, L., Zhang, Q., and Anastasio, C.: Secondary Organic Aerosol Production from Aqueous Reactions of Atmospheric Phenols with an Organic Triplet Excited State, Environ. Sci. Technol., 48, 1049-1057, https://doi.org/10.1021/es4045715, 2014.

Song, J., Li, M., Jiang, B., Wei, S., Fan, X., and Peng, P. a.: Molecular Characterization of Water-Soluble Humic like Substances in Smoke Particles Emitted from Combustion of Biomass Materials and Coal Using Ultrahigh-Resolution Electrospray Ionization Fourier Transform Ion Cyclotron Resonance Mass Spectrometry, Environ. Sci. Technol., 52, 2575-2585, https://doi.org/10.1021/acs.est.7b06126, 2018.

Song, J., Li, M., Zou, C., Cao, T., Fan, X., Jiang, B., Yu, Z., Jia, W., and Peng, P. a.: Molecular Characterization of Nitrogen-Containing Compounds in Humic-like Substances Emitted from Biomass Burning and Coal Combustion, Environ. Sci. Technol., 56, 119-130, https://doi.org/10.1021/acs.est.1c04451, 2022.

Stolzenburg, D., Fischer, L., Vogel, A. L., Heinritzi, M., Schervish, M., Simon, M., Wagner, A. C., Dada, L., Ahonen, L. R., Amorim, A., Baccarini, A., Bauer, P. S., Baumgartner, B., Bergen, A., Bianchi, F., Breitenlechner, M., Brilke, S., Buenrostro Mazon, S., Chen, D., Dias, A., Draper, D. C., Duplissy, J., El Haddad, I., Finkenzeller,

H., Frege, C., Fuchs, C., Garmash, O., Gordon, H., He, X., Helm, J., Hofbauer, V., Hoyle, C. R., Kim, C., Kirkby, J., Kontkanen, J., Kürten, A., Lampilahti, J., Lawler, M., Lehtipalo, K., Leiminger, M., Mai, H., Mathot, S., Mentler, B., Molteni, U., Nie, W., Nieminen, T., Nowak, J. B., Ojdanic, A., Onnela, A., Passananti, M., Petäjä, T., Quéléver, L. L. J., Rissanen, M. P., Sarnela, N., Schallhart, S., Tauber, C., Tomé, A., Wagner, R., Wang, M., Weitz, L., Wimmer, D., Xiao, M., Yan, C., Ye, P., Zha, Q., Baltensperger, U., Curtius, J., Dommen, J., Flagan, R. C., Kulmala, M., Smith, J. N., Worsnop, D. R., Hansel, A., Donahue, N. M., and Winkler, P. M.: Rapid growth of organic aerosol nanoparticles over a wide tropospheric temperature range, P. Natl. Acad. Sci. USA, 115, 9122-9127, https://doi.org/10.1073/pnas.1807604115, 2018.

Su, S., Xie, Q., Lang, Y., Cao, D., Xu, Y., Chen, J., Chen, S., Hu, W., Qi, Y., Pan, X., Sun, Y., Wang, Z., Liu, C.-Q., Jiang, G., and Fu, P.: High Molecular Diversity of Organic Nitrogen in Urban Snow in North China, Environ. Sci. Technol., 55, 4344-4356, https://dx.doi.org/10.1021/acs.est.0c06851, 2021.

Surratt, J. D., Chan, A. W. H., Eddingsaas, N. C., Chan, M., Loza, C. L., Kwan, A. J., Hersey, S. P., Flagan, R. C., Wennberg, P. O., and Seinfeld, J. H.: Reactive intermediates revealed in secondary organic aerosol formation from isoprene, P. Natl. Acad. Sci. USA, 107, 6640-6645, https://doi.org/10.1073/pnas.0911114107, 2010.

Tomsche, L., Piel, F., Mikoviny, T., Nielsen, C. J., Guo, H., Campuzano-Jost, P., Nault, B. A., Schueneman, M. K., Jimenez, J. L., Halliday, H., Diskin, G., DiGangi, J. P., Nowak, J. B., Wiggins, E. B., Gargulinski, E., Soja, A. J., and Wisthaler, A.: Measurement report: Emission factors of NH3 and NHx for wildfires and agricultural

816 fires in the United States, Atmos. Chem. Phys., 23, 2331-2343,
817 https://doi.org/10.5194/acp-23-2331-2023, 2023.
818 W. Hogg, R. and T. Gillan, F.: Fatty acids, sterols and hydrocarbons in the leaves
819 from eleven species of mangrove, Phytochemistry, 23, 93-97,
820 https://doi.org/10.1016/0031-9422(84)83084-8, 1984.
821 Wan, X., Qin, F., Cui, F., Chen, W., Ding, H., and Li, C.: Correlation between the
822 distribution of solar energy resources and the cloud cover in Xinjiang, IOP Conf. Ser.:
823 Earth Environ. Sci., 675, 012060, https://doi.org/10.1088/1755-1315/675/1/012060,
824 2021.
825 Wang, H., Wang, Q., Gao, Y., Zhou, M., Jing, S., Qiao, L., Yuan, B., Huang, D.,
826 Huang, C., Lou, S., Yan, R., de Gouw, J. A., Zhang, X., Chen, J., Chen, C., Tao, S., An,
827 J., and Li, Y.: Estimation of Secondary Organic Aerosol Formation During a
828 Photochemical Smog Episode in Shanghai, China, J. Geophys. Res.-Atmos., 125,
829 e2019JD032033, https://doi.org/10.1029/2019JD032033, 2020.
830 Wang, K., Huang, R.-J., Brueggemand, M., Zhang, Y., Yang, L., Ni, H., Guo, J.,
831 Wang, M., Han, J., Bilde, M., Glasius, M., and Hoffmann, T.: Urban organic aerosol
832 composition in eastern China differs from north to south: molecular insight from a
833 liquid chromatography-mass spectrometry (Orbitrap) study, Atmos. Chem. Phys., 21,
834 9089-9104, https://doi.org/10.5194/acp-21-9089-2021, 2021a.
835 Wang, L., Zhang, K., Huang, W., Han, W., and Tian, C.-Y.: Seed oil content and
836 fatty acid composition of annual halophyte Suaeda acuminata: A comparative study on
837 dimorphic seeds, Afr. J. Biotechnol., 10, 19106-19108,

https://doi.org/10.5897/ajb11.2597, 2011.

Wang, Q., Shao, M., Zhang, Y., Wei, Y., Hu, M., and Guo, S.: Source apportionment of fine organic aerosols in Beijing, Atmos. Chem. Phys., 9, 8573-8585, https://doi.org/10.5194/acp-9-8573-2009, 2009.

Wang, X., Hayeck, N., Brüggemann, M., Yao, L., Chen, H., Zhang, C., Emmelin, C., Chen, J., George, C., and Wang, L.: Chemical Characteristics of Organic Aerosols in Shanghai: A Study by Ultrahigh-Performance Liquid Chromatography Coupled With Orbitrap Mass Spectrometry, J. Geophys. Res.-Atmos., 122, 11,703-711,722, https://doi.org/10.1002/2017JD026930, 2017a.

Wang, X., Shen, Z., Liu, F., Lu, D., Tao, J., Lei, Y., Zhang, Q., Zeng, Y., Xu, H., Wu, Y., Zhang, R., and Cao, J.: Saccharides in summer and winter $PM_{2.5}$ over Xi'an, Northwestern China: Sources, and yearly variations of biomass burning contribution to $PM_{2.5}$, Atmos. Res., 214, 410-417, https://doi.org/10.1016/j.atmosres.2018.08.024, 2018.

Wang, Y., Zhao, Y., Li, Z., Li, C., Yan, N., and Xiao, H.: Importance of Hydroxyl Radical Chemistry in Isoprene Suppression of Particle Formation from α-Pinene Ozonolysis, ACS Earth Space Chem., 5, 487-499, https://doi.org/10.1021/acsearthspacechem.0c00294, 2021b.

Wang, Y., Hu, M., Lin, P., Guo, Q., Wu, Z., Li, M., Zeng, L., Song, Y., Zeng, L., Wu, Y., Guo, S., Huang, X., and He, L.: Molecular Characterization of Nitrogen-Containing Organic Compounds in Humic-like Substances Emitted from Straw Residue Burning, Environ. Sci. Technol., 51, 5951-5961,

https://doi.org/10.1021/acs.est.7b00248, 2017b.

Wang, Y., Hu, M., Hu, W., Zheng, J., Niu, H., Fang, X., Xu, N., Wu, Z., Guo, S., Wu, Y., Chen, W., Lu, S., Shao, M., Xie, S., Luo, B., and Zhang, Y.: Secondary Formation of Aerosols Under Typical High-Humidity Conditions in Wintertime Sichuan Basin, China: A Contrast to the North China Plain, J. Geophys. Res.-Atmos., 126, e2021JD034560, https://doi.org/10.1029/2021JD034560, 2021c.

Xie, Q., Su, S., Chen, S., Xu, Y., Cao, D., Chen, J., Ren, L., Yue, S., Zhao, W., Sun, Y., Wang, Z., Tong, H., Su, H., Cheng, Y., Kawamura, K., Jiang, G., Liu, C. Q., and Fu, P.: Molecular characterization of firework-related urban aerosols using Fourier transform ion cyclotron resonance mass spectrometry, Atmos. Chem. Phys., 20, 6803-6820, https://doi.org/10.5194/acp-20-6803-2020, 2020.

Xu, Y. and Xiao, H.: Concentrations and nitrogen isotope compositions of free amino acids in Pinus massoniana (Lamb.) needles of different ages as indicators of atmospheric nitrogen pollution, Atmos. Environ., 164, 348-359, https://doi.org/10.1016/j.atmosenv.2017.06.024, 2017.

Xu, Y., Lin, Z., and Wu, C.: Spatiotemporal Variation of the Burned Area and Its Relationship with Climatic Factors in Central Kazakhstan, Remote Sens., 13, 313, https://doi.org/10.3390/rs13020313, 2021.

Xu, Y., Dong, X.-N., Xiao, H.-Y., He, C., and Wu, D.-S.: Water-Insoluble Components in Rainwater in Suburban Guiyang, Southwestern China: A Potential Contributor to Dissolved Organic Carbon, J. Geophys. Res.-Atmos., 127, e2022JD037721, https://doi.org/10.1029/2022JD037721, 2022a.

Xu, Y., Dong, X.-N., Xiao, H.-Y., Zhou, J.-X., and Wu, D.-S.: Proteinaceous Matter and Liquid Water in Fine Aerosols in Nanchang, Eastern China: Seasonal Variations, Sources, and Potential Connections, J. Geophys. Res.-Atmos., 127, e2022JD036589, https://doi.org/10.1029/2022JD036589, 2022b.

Xu, Y., Dong, X. N., He, C., Wu, D. S., Xiao, H. W., and Xiao, H. Y.: Mist cannon trucks can exacerbate the formation of water-soluble organic aerosol and $PM_{2.5}$ pollution in the road environment, Atmos. Chem. Phys., 23, 6775-6788, https://doi.org/10.5194/acp-23-6775-2023, 2023.

Xu, Y., Miyazaki, Y., Tachibana, E., Sato, K., Ramasamy, S., Mochizuki, T., Sadanaga, Y., Nakashima, Y., Sakamoto, Y., Matsuda, K., and Kajii, Y.: Aerosol Liquid Water Promotes the Formation of Water-Soluble Organic Nitrogen in Submicrometer Aerosols in a Suburban Forest, Environ. Sci. Technol., 54, 1406-1414, https://dx.doi.org/10.1021/acs.est.9b05849, 2020.

Yang, T., Xu, Y., Ye, Q., Ma, Y. J., Wang, Y. C., Yu, J. Z., Duan, Y. S., Li, C. X., Xiao, H. W., Li, Z. Y., Zhao, Y., and Xiao, H. Y.: Spatial and diurnal variations of aerosol organosulfates in summertime Shanghai, China: potential influence of photochemical processes and anthropogenic sulfate pollution, Atmos. Chem. Phys., 23, 13433-13450, https://doi.org/10.5194/acp-23-13433-2023, 2023.

Zahardis, J., Geddes, S., and Petrucci, G. A.: The ozonolysis of primary aliphatic amines in fine particles, Atmos. Chem. Phys., 8, 1181-1194, https://doi.org/10.5194/acp-8-1181-2008, 2008.

Zarzana, K. J., De Haan, D. O., Freedman, M. A., Hasenkopf, C. A., and Tolbert,

M. A.: Optical Properties of the Products of α-Dicarbonyl and Amine Reactions in Simulated Cloud Droplets, Environ. Sci. Technol., 46, 4845-4851, https://doi.org/10.1021/es2040152, 2012.

Zeng, Y., Ning, Y., Shen, Z., Zhang, L., Zhang, T., Lei, Y., Zhang, Q., Li, G., Xu, H., Ho, S. S. H., and Cao, J.: The Roles of N, S, and O in Molecular Absorption Features of Brown Carbon in PM2.5 in a Typical Semi-Arid Megacity in Northwestern China, J. Geophys. Res.-Atmos., 126, e2021JD034791, https://doi.org/10.1029/2021JD034791, 2021.

Zeng, Y., Shen, Z., Takahama, S., Zhang, L., Zhang, T., Lei, Y., Zhang, Q., Xu, H., Ning, Y., Huang, Y., Cao, J., and Rudolf, H.: Molecular Absorption and Evolution Mechanisms of PM2.5 Brown Carbon Revealed by Electrospray Ionization Fourier Transform–Ion Cyclotron Resonance Mass Spectrometry During a Severe Winter Pollution Episode in Xi'an, China, Geophys. Res. Lett., 47, e2020GL087977, https://doi.org/10.1029/2020GL087977, 2020.

Zhang, B., Shen, Z., He, K., Sun, J., Huang, S., Xu, H., Li, J., Ho, S. S. H., and Cao, J.-j.: Insight into the Primary and Secondary Particle-Bound Methoxyphenols and Nitroaromatic Compound Emissions from Solid Fuel Combustion and the Updated Source Tracers, Environ. Sci. Technol., 57, 14280-14288, 10.1021/acs.est.3c04370, 2023.

Zhang, Q., Jimenez, J. L., Canagaratna, M. R., Allan, J. D., Coe, H., Ulbrich, I., Alfarra, M. R., Takami, A., Middlebrook, A. M., Sun, Y. L., Dzepina, K., Dunlea, E., Docherty, K., DeCarlo, P. F., Salcedo, D., Onasch, T., Jayne, J. T., Miyoshi, T., Shimono,

A., Hatakeyama, S., Takegawa, N., Kondo, Y., Schneider, J., Drewnick, F., Borrmann, S., Weimer, S., Demerjian, K., Williams, P., Bower, K., Bahreini, R., Cottrell, L., Griffin, R. J., Rautiainen, J., Sun, J. Y., Zhang, Y. M., and Worsnop, D. R.: Ubiquity and dominance of oxygenated species in organic aerosols in anthropogenically-influenced Northern Hemisphere midlatitudes, Geophys. Res. Lett., 34, https://doi.org/10.1029/2007GL029979, 2007.

Zhang, T., Shen, Z., Huang, S., Lei, Y., Zeng, Y., Sun, J., Zhang, Q., Ho, S. S. H., Xu, H., and Cao, J.: Optical properties, molecular characterizations, and oxidative potentials of different polarity levels of water-soluble organic matters in winter PM2.5 in six China's megacities, Sci. Total Environ., 853, 158600, https://doi.org/10.1016/j.scitotenv.2022.158600, 2022.

Zhao, Y., Hu, M., Slanina, S., and Zhang, Y.: Chemical Compositions of Fine Particulate Organic Matter Emitted from Chinese Cooking, Environ. Sci. Technol., 41, 99-105, https://doi.org/10.1021/es0614518, 2007.

Zhong, S., Chen, S., Deng, J., Fan, Y., Zhang, Q., Xie, Q., Qi, Y., Hu, W., Wu, L., Li, X., Pavuluri, C. M., Zhu, J., Wang, X., Liu, D., Pan, X., Sun, Y., Wang, Z., Xu, Y., Tong, H., Su, H., Cheng, Y., Kawamura, K., and Fu, P.: Impact of biogenic secondary organic aerosol (SOA) loading on the molecular composition of wintertime $PM_{2.5}$ in urban Tianjin: an insight from Fourier transform ion cyclotron resonance mass spectrometry, Atmos. Chem. Phys., 23, 2061-2077, https://doi.org/10.5194/acp-23-2061-2023, 2023.

Zhou, S., Guo, F., Chao, C.-Y., Yoon, S., Alvarez, S. L., Shrestha, S., Flynn, J. H.,

III, Usenko, S., Sheesley, R. J., and Griffin, R. J.: Marine Submicron Aerosols from the Gulf of Mexico: Polluted and Acidic with Rapid Production of Sulfate and Organosulfates, Environ. Sci. Technol., 57, 5149-5159, https://doi.org/10.1021/acs.est.2c05469, 2023.

Zou, C., Cao, T., Li, M., Song, J., Jiang, B., Jia, W., Li, J., Ding, X., Yu, Z., Zhang, G., and Peng, P.: Measurement report: Changes in light absorption and molecular composition of water-soluble humic-like substances during a winter haze bloom-decay process in Guangzhou, China, Atmos. Chem. Phys., 23, 963-979, https://doi.org/10.5194/acp-23-963-2023, 2023.

Figure 1.

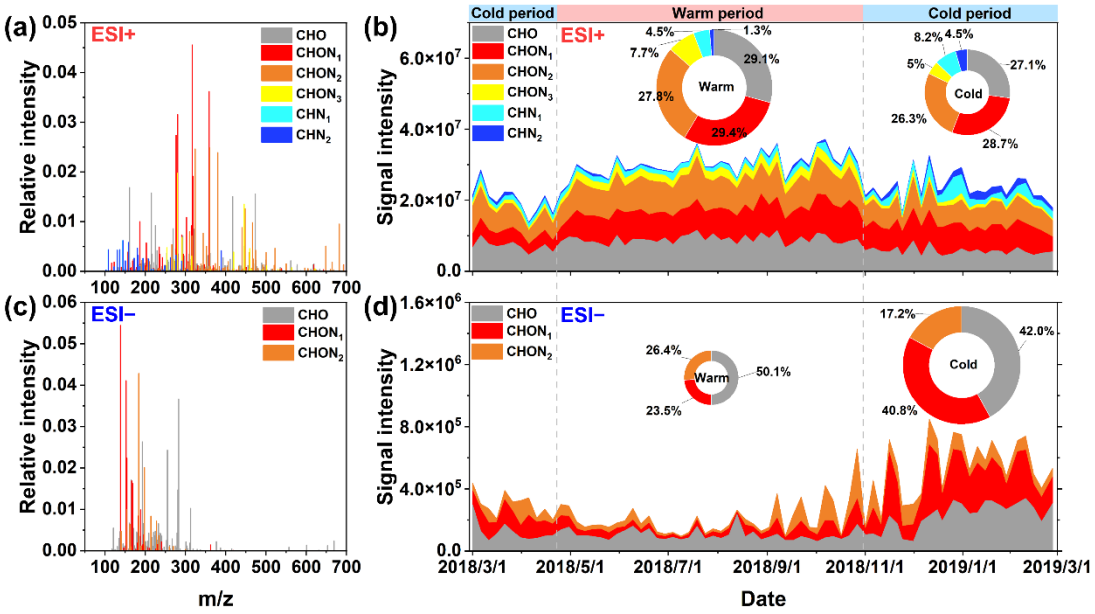

Figure 1. The reconstructed mass spectrum distribution of the detected species in $PM_{2.5}$ in (**a**) ESI+ and (**c**) ESI− modes during the whole campaign. Temporal variations in the fractional distribution of classified compounds in (**b**) ESI+ and (**d**) ESI− modes. The ring diagrams inside the panel show the signal intensity fractions of classified compounds, the size of which is proportional to the total signal intensity of all species detected in $PM_{2.5}$ in different periods.

Figure 2.

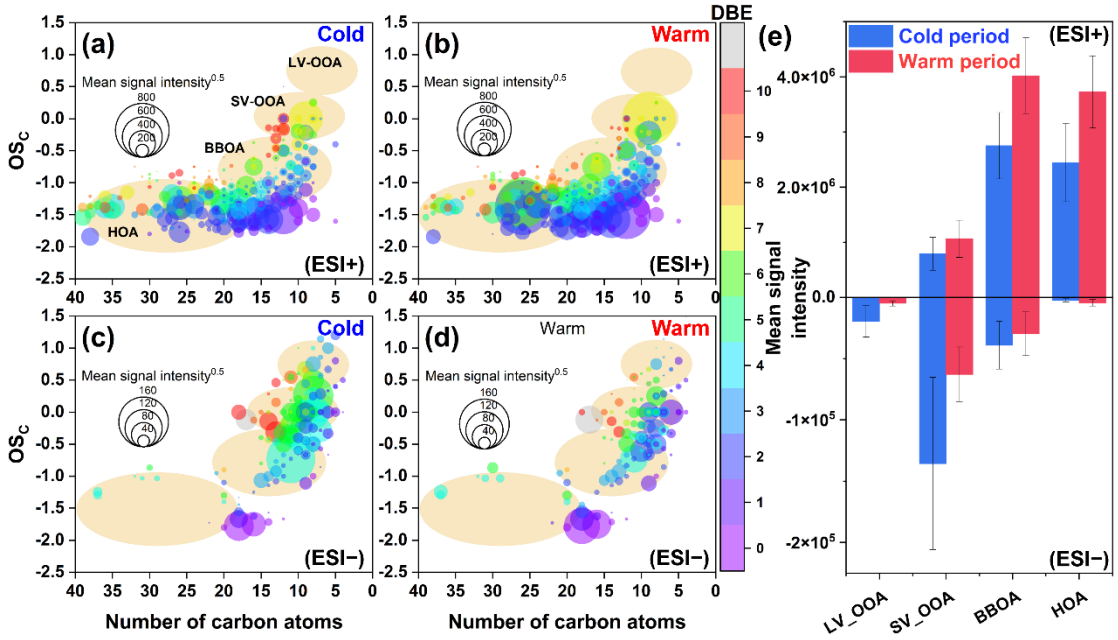

Figure 2. OSc values of CHO molecules detected in (**a** and **b**) ESI+ and (**c** and **d**) ESI− modes in $PM_{2.5}$ collected from different periods (cold vs. warm). The size and color of the circle indicate the mean signal intensity and DBE value of compounds, respectively. The light-orange background indicates the areas of LV-OOA, SV-OOA, BBOA, and HOA (Kroll et al., 2011), according to which (**e**) the mean signal intensity of classified compounds was calculated for samples from different periods.

Figure 3

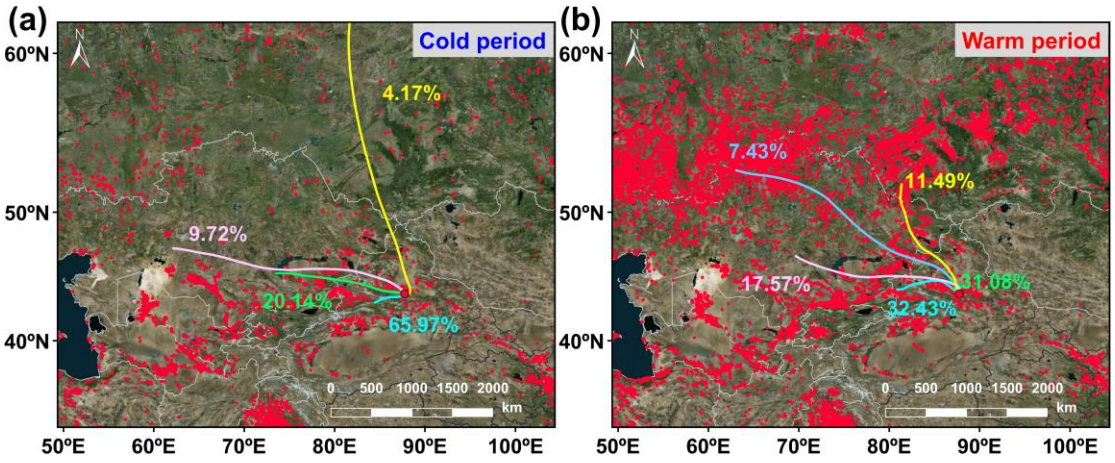

Figure 3. The 3-day (72 h) back trajectories illustrating the typical air mass flows to the study site during the (a) warm and (b) cool periods. Fire spots were shown in red, which was created based on NASA active fire data (VIIRS 375 m, https://firms.modaps.eosdis.nasa.gov/active_fire/). The map was derived from ©MeteoInfoMap (version 3.6.2) (Chinese Academy of Meteorological Sciences, China).

Figure 4.

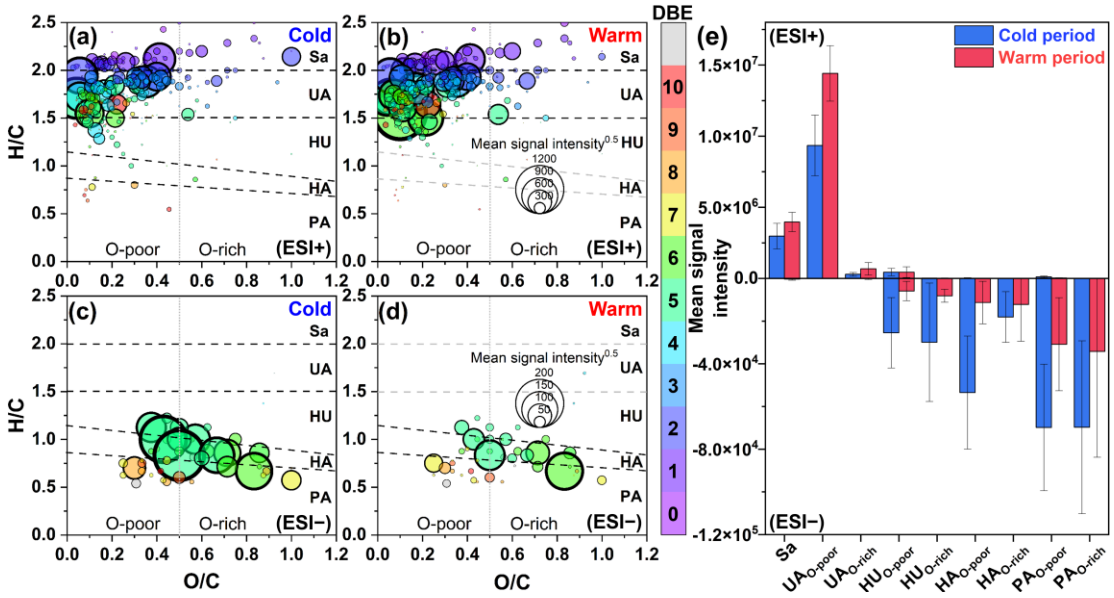

Figure 4. Van Krevelen diagrams of CHON molecules detected in (**a** and **b**) ESI+ and (**c** and **d**) ESI− modes in $PM_{2.5}$ collected from different periods (cold vs. warm). The subgroups in the panel include saturated-like (Sa), unsaturated aliphatic-like (UA), highly unsaturated-like (HU), highly aromatic-like (HA), and polycyclic aromatic-like (PA) compounds, further distinguishing between oxygen-poor and oxygen-rich compounds with an oxygen to carbon ratio of 0.5. The size and color of the circle indicate the mean signal intensity and DBE value of compounds, respectively. The (**e**) mean signal intensity of classified compounds was calculated for samples from different periods.

Figure 5.

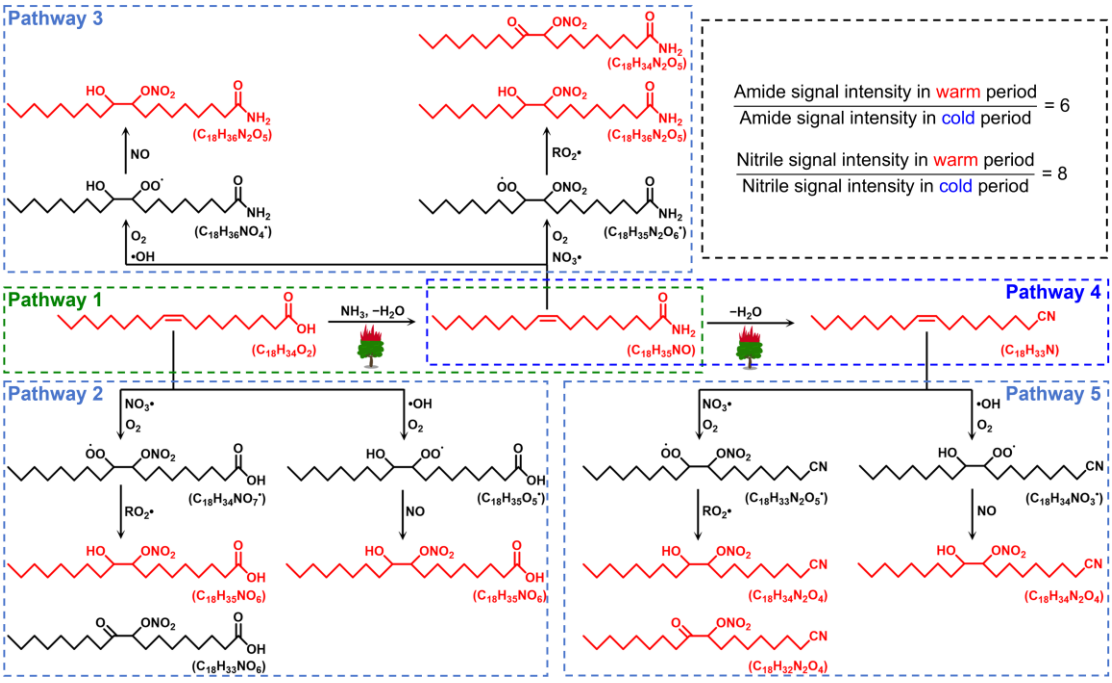

Figure 5. Proposed pathways for the reactions of carboxylic acids (oleic acid as a representative) with reactive nitrogen and atmospheric oxides to form the observed NOCs in $PM_{2.5}$ under the influence of the high temperature generated during wildfires or forest fires. Compounds observed in $PM_{2.5}$ were shown in red.

Figure 6.

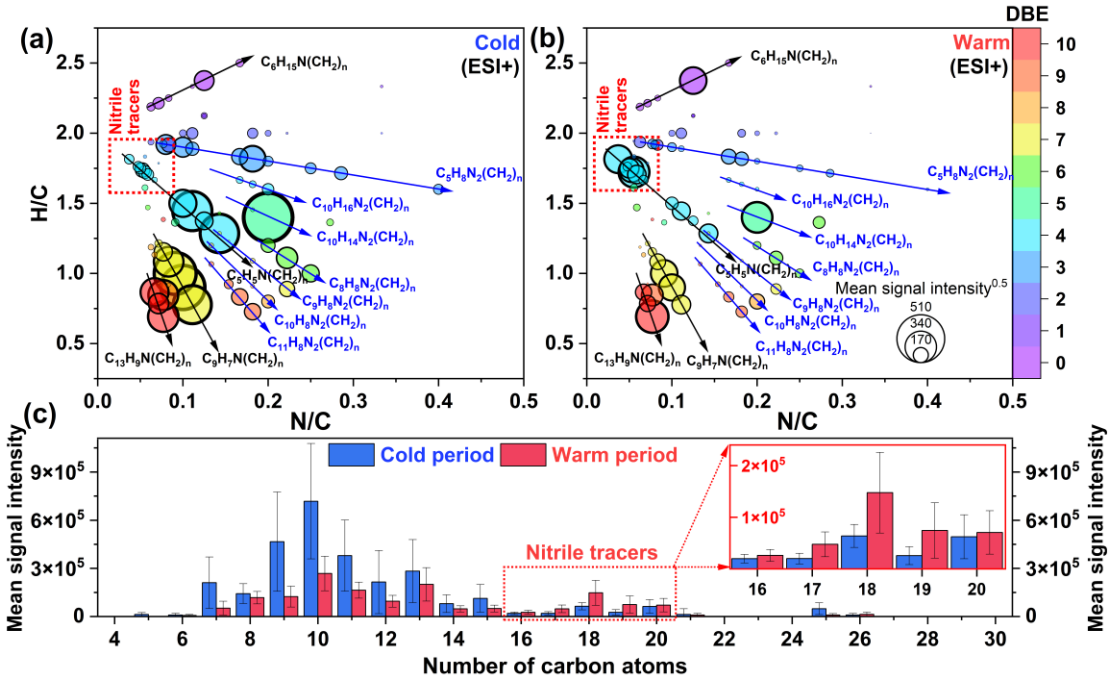

Figure 6. Van Krevelen diagrams of CHN molecules detected in $PM_{2.5}$ collected from the (**a**) cold and (**b**) warm periods. The size and color of the circle indicate the mean signal intensity and DBE value of compounds, respectively. The mean signal intensity distributions of (**c**) carbon atoms in CHN molecules detected in $PM_{2.5}$ collected from the cold and warm periods

1022 **Figure 7.**

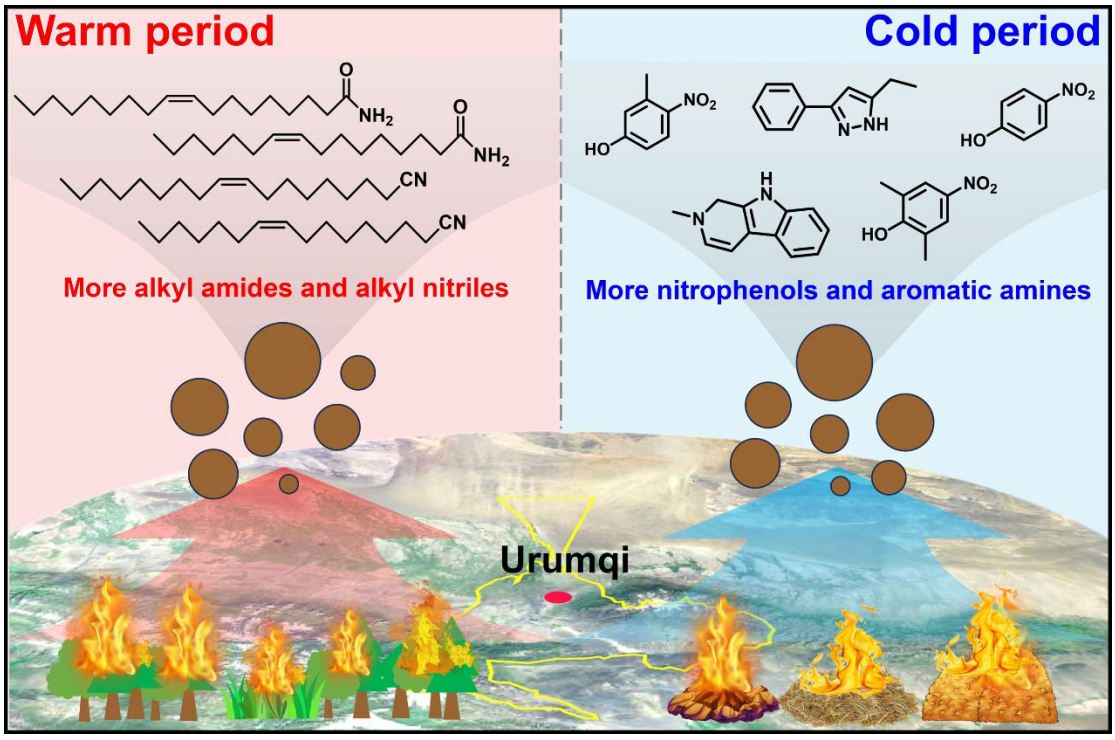

1023

1024 **Figure 7.** Conceptual picture showing the differential impacts of combustion of fresh

1025 and old-age biomass materials on aerosol NOCs in suburban Urumqi. The map was

1026 derived from ©Baidu Maps (BIDU, China).